Redox Behavior of $Y_{0.05}Ce_{0.1}Zr_{0.85}O_2$ and $Y_{0.1}Ce_{0.1}Zr_{0.8}O_2$ System Catalysts Doped with Copper(II)

S. P. Kulyova, E. V. Lunina,† V. V. Lunin, B. G. Kostyuk, G. P. Muravyova, and A. N. Kharlanov

Chemistry Department of Moscow State University, Moscow, Russia

E. A. Zhilinskaya and A. Aboukaïs*

Laboratoire de Catalyse et Environnement, EA 2598, MREID, Université du Littoral Côte d'Opale, 145, Av. Maurice Schumann, 59140 Dunkerque Cedex, France

Received August 4, 2000. Revised Manuscript Received January 19, 2001

The redox behavior of $Y_{0.05}Ce_{0.1}Zr_{0.85}O_2$ and $Y_{0.1}Ce_{0.1}Zr_{0.8}O_2$ doped with copper(II) was studied by means of diffuse reflectance electronic spectra **(**DRES), temperature-programmed reduction (TPR), and electron paramagnetic resonance (EPR) techniques. In the absence of copper, it has been demonstrated that the solid is more reducible while it contains more yttrium. The addition of copper in the form of isolated or clusters/small particles makes the reduction of Ce^{4+} ions present on the solid surface and in the bulk easier. Nevertheless, three types of Cu^{2+} ions were evidenced in the solids: isolated and cluster species in strong dipolar interaction with octahedral symmetries and tetragonal distortion surrounded by more than six ligands, aggregates of CuO located on the solid surface, and finally isolated Cu^{2+} ions located in the solid bulk with octahedral symmetries and strong distortions and which remain silent toward reduction by CO.

Introduction

The operating conditions of catalysts for automotive exhaust control (three-way catalysts, TWCs) essentially differ from those of the majority of industrial catalysts. These differences are related to unsteady-state parameters of gas flow,[1,2] first of all, with fluctuations of composition of exhaust gases directed onto the catalyst. The inconstancy of gas flow composition is explained by its dependence on the air-to-fuel ratio (A/F) in cylinders of an engine, which in turn, varies over a wide range because of change in the driving style and speed.[1−2]

For optimum TWC performances "an oxygen storage component" (for example, CeO_2) is introduced in the catalyst. It is well-known that CeO_2 is able to act as an efficient oxygen buffer by releasing/storing O_2 because of its capability of undergoing effective reduction and reoxidation under rich (A/F < 1) and lean (A/F > 1) conditions, respectively.[2−5] Thus, the decrease in sensitivity of Ce-containing TWCs to oscillations of a gas mixture composition and, consequently, enhancement of their redox properties occur because of compensation of gas composition fluctuations by high mobility of lattice oxygen in CeO_2.

In addition, it is known that the introduction of ZrO_2 into the CeO_2 framework with the formation of a solid solution results in a structural modification of the CeO_2 lattice, which makes bulk oxygen highly mobile. The reason for the increased lattice oxygen mobility lays in the highly defective structure and lattice strain, which are generated by insertion of the smaller isovalent Zr^{4+} cations into the CeO_2 lattice (0.84 and 0.97 Å for Zr^{4+} and Ce^{4+}, respectively).[3,6] Maximal quantity of structural defects is realized for binary solid solutions of cubic symmetry and not less than 50% of CeO_2 is required for the stabilization of such a structure.[4,6,7]

The Y_2O_3−CeO_2−ZrO_2 solid solutions[3,6−8] high oxygen storage capacity (OSC) in combination with thermal stability and excellent mechanical properties makes these materials, from this perspective, supports for TWC. Indeed, it was shown that the insertion of 2.5−5 mol % of a trivalent cation (such as Y^{3+}) in the $60CeO_2$−$40ZrO_2$ lattice promotes the stabilization of a single homogeneous cubic phase, increases the ability of the solid to accumulate oxygen, and improves oxygen exchange at low temperatures (close to those that are characteristic of cold-start conditions).

The purpose of this work is to investigate the reducibility of Cu-containing $Y_{0.05}Ce_{0.1}Zr_{0.85}O_2$ and $Y_{0.1}Ce_{0.1}Zr_{0.8}O_2$ systems and to determine the nature of the copper species (valence and phase states, environmental symmetry) that are present in the solids.

* To whom correspondence should be addressed
† Deceased.

(1) Kirchner, T.; Eigenberger, G. *Catal. Today* **1997**, *38*, 3.
(2) Tagliaferri, S.; Köppel, R. A.; Baiker, A. *Appl. Catal. B* **1998**, *15*, 159.
(3) Kašpar, J.; Fornasiero, P.; Graziani, M. *Catal. Today* **1999**, *50*, 285.
(4) Nibbelke, R. H.; Nievergeld, A. J. L.; Hoebink, J. H. B. J.; Marin, G. B. *Appl. Catal. B* **1998**, *19*, 245.
(5) González-Velasco, J. R.; Gutiérrez-Ortiz, M. A.; Marc, J. L.; Botas, J. A.; Gonzalez-Marcos, M. P.; Blanchard, G. *Appl. Catal. B* **1999**, *22*, 167.
(6) Di Monte, R.; Fornasiero, P.; Graziani, M.; Kašpar, J. *J. Alloys Compd.* **1998**, *275−277*, 877.
(7) Vidmar, P.; Fornasiero, P.; Kašpar, J.; Gubitosa, G.; Graziani, M. *J. Catal.* **1997**, *171*, 160.
(8) Hori, C. E.; Permana, H.; Ng, K. Y. S.; Brenner, A.; More, K.; Rahmoeller, K. M.; Belton, D. *Appl. Catal. B* **1998**, *16*, 105.

10.1021/cm000636p CCC: $20.00
Published on Web 04/26/2001

Experimental Section

Complex oxide compositions $Y_xCe_{0.1}Zr_{0.9-x}O_2$ ($x = 0.5$ and 1.0) were prepared by coprecipitation of Y, Ce, and Zr hydroxides by means of adding ammonia hydroxide to a solution of a mixture of nitrates ($C = 0.2$ M) at the desired Y/Ce/Zr ratio (pH = 10.5−11). The prepared gel was washed with deionized water, dried in air at room temperature (T_R) (24 h) and then in air at 373−393 K (5 h), and after, calcined at 823 K (5 h) in a muffle furnace.

The $Y_{0.05}Ce_{0.1}Zr_{0.85}O_2$ and $Y_{0.1}Ce_{0.1}Zr_{0.8}O_2$ solid solutions were impregnated by the copper cations (using copper nitrate solution) with the subsequent drying in air at 373−393 K (5 h) and calcining at 523 K (3 h). Powder X-ray diffraction patterns (XRD) were recorded on a DRON-3M diffractometer using Ni-filtered Cu Kα radiation ($\lambda = 1.5418$ Å). The mean crystallite size (D) of the samples was determined through an X-ray diffraction line broadening method using the Scherrer equation: $D = (K\lambda/\beta \cos \theta)$, where λ is the X-ray wavelength, K is the particle shape factor, taken as 0.94, and β is the full width at half-maximum of the peak at 2θ.

Temperature-programmed reduction (TPR) of samples was carried out in a flow device equipped with a system of gas preparation and purification, a quartz reactor and a tube furnace, and a thermal conductivity detector (TCD). Before the TPR measurements, the solids were calcined at 673 K under a flow of dried air for 1 h. A typical reduction was performed in a mixture of 5 vol % H_2 in Ar. The flow rate was 23 mL/min and the heating rate 13.2 K min^{-1}. H_2 consumption was estimated by comparison of the integrated peak areas with those obtained for the standard (NiO). Integration was performed after the correction of the baseline of each TPR peak. The area of the TPR peak (related to quantity of labile oxygen) and the temperature of maximal reduction (characteristic of oxygen mobility) were chosen as parameters used for interpretation of TPR data on the redox properties of the solids.

EPR spectra were recorded at 293 and 77 K on a EMX Bruker spectrometer operating in the X-band frequency (9.3 GHz) and using 100-kHz modulation. The g values were determined by measuring the magnetic field, H, and the microwave frequency.

Diffuse reflectance electronic spectra (DRES) were recorded with a spectrophotometer of UV−vis range, Specord M40. The registration of the spectra was carried out at the T_R in air. Barium sulfate was used as a reference.

Diffuse reflectance spectra of adsorbed CO were recorded using a spectrophotometer of infrared range, Specord M80. The sample (0.25−0.5 mm) was placed in a quartz ampule (with CaF_2 window), which was put in a holder of the spectrophotometer.

Results and Discussion

1. $Y_xCe_{0.1}Zr_{0.9-x}O_2$ Supports. 1.1. XRD. Pure CeO_2 has the fluorite (CaF_2) structure.[9] Insertion of ZrO_2 into the CeO_2 framework with the formation of a solid solution strongly modifies the oxygen sublattice. So the number of oxygens around Zr^{4+} decreases from 8 to 6 because of the displacement of two oxygen ions from the positions, which they would have in the ideal fluorite structure.[10] The perturbation of the Zr−O coordination sphere leads to highly disordered oxygen in the lattice, having enhanced mobility. Fornasiero et al.[11] have shown that the order/disorder of the oxygen sublattice, generated by insertion of ZrO_2 into the CeO_2 lattice, is indicated as a key factor in promoting reduction in the majority of these mixed oxides. Significant differences are found between the Zr−O bonding in materials derived from a high-surface-area mixed oxide and the sintered ceramic-type mixed oxides, as the coordination number decreases from 7 to 6. Apparently, the more defective the structure, the higher the mobility of oxygen in the bulk of the solid.

It is known[3,6,7,11−13] that a large amount of CeO_2 (40−60 mol %) is required for the stabilization of the most defective cubic structure. According to ref 14, the addition of Y^{3+} stabilizes the cubic structure of ternary systems at very low content of both yttrium and cerium oxide (less than 10 mol %). It was also reported[3,6,7] that insertion of a trivalent additive (e.g., Y^{3+}) in the CeO_2−ZrO_2 lattice favors stabilization of a single homogeneous cubic phase, increases the ability of the solid to accumulate oxygen, and improves oxygen exchange at low temperatures (close to those characteristic of cold-start conditions). Besides, the addition of Y^{3+} into the CeO_2−ZrO_2 framework increases the strength and hardness of these materials.[15]

Considering probable formation of a tetragonal and/or cubic ternary solid solution,[7] we investigated the influence of the amount of inserted Y^{3+} on phase transformations of $10CeO_2$−$90ZrO_2$, which is of special interest in choosing a support of optimal composition. It is worth noting that ZrO_2 should be the dominant factor determining the nature of the available phase as all the samples are characterized by the high content of zirconium (from 80 to 90 mol %). According to the ASTM database, the single peaks are observed at the angles of about 35°, 50°, and 60° (2 Å) for the cubic phase of the macrocomponent, while the doublets present on the diffractogram of tetragonal ZrO_2 in the same angular ranges.

Figure 1a shows the powder X-ray patterns of the $Y_{0.05}Ce_{0.1}Zr_{0.85}O_2$ sample calcined at 823 K. The broad diffraction peaks of as-prepared samples are attributed to the presence of small crystallites formed after calcination. The width of these peaks, which decreased after calcination at 1743 K (Figure 1b), demonstrated that the average particle size of the solids was increased.

The XRD pattern of the $Y_{0.05}Ce_{0.1}Zr_{0.85}O_2$ solid shows strong splitting of the peaks at about $2\theta = 35°$, 50°, and 60°. A similar phenomenon was obtained by other authors,[7] indicating then the presence of a mixture of tetragonal and cubic phases in the solid. The depth of the peak splitting disappeared for the $Y_{0.1}Ce_{0.1}Zr_{0.8}O_2$ solid (Figure 1c). This suggests that with an increase of the yttrium concentration the formation of a single cubic phase is favored. This single phase for the $Y_{0.1}Ce_{0.1}Zr_{0.8}O_2$ sample is indexed in the $Fm3m$ space group. The cell parameter was calculated as 5.167 Å. The crystallite sizes of $Y_{0.05}Ce_{0.1}Zr_{0.85}O_2$ and $Y_{0.1}Ce_{0.1}Zr_{0.8}O_2$ samples were evaluated at 11 and 10 nm, respectively. This slight difference obtained is due to the presence of a small amount of the tetragonal

(9) Trovarelli, A. *Catal. Rev.-Sci. Eng.* **1996**, *38*(4), 439.
(10) Vlaic, G.; Fornasiero, P.; Geremia, S.; Kašpar, J.; Graziani, M. *J. Catal.* **1997**, *168*, 386.
(11) Fornasiero, P.; Fonda, E.; Di Monte, R.; Vlaic, G.; Kašpar, J.; Graziani, M. *J. Catal.* **1999**, *187*, 177.
(12) Fornasiero, P.; Balducci, G.; Di Monte, R.; Kašpar, J.; Sergo, V.; Gubitosa, G.; Ferrero, A.; Graziani, M. *J. Catal.* **1996**, *164*, 173.
(13) Fornasiero, P.; Di Monte, R.; Ranga Rao, G.; Kašpar, J.; Meriani, S.; Trovarelli, A.; Graziani, M. *J. Catal.* **1995**, *151*, 168.
(14) Markaryan, G. L.; Ikryannikova, L. N.; Muravieva, G. P.; Turakulova, A. O.; Kostyuk, B. G.; Lunina, E. V.; Lunin, V. V.; Zhilinskaya, E.; Aboukaïs, A. *Colloids Surf. A* **1999**, *151*, 435.
(15) Oh, H. S.; Lee, Y. B.; Kim, Y. W.; Oh, K. D.; Park, H. C. *Yoop Hakhoechi* **1997**, *34*(1), 102.

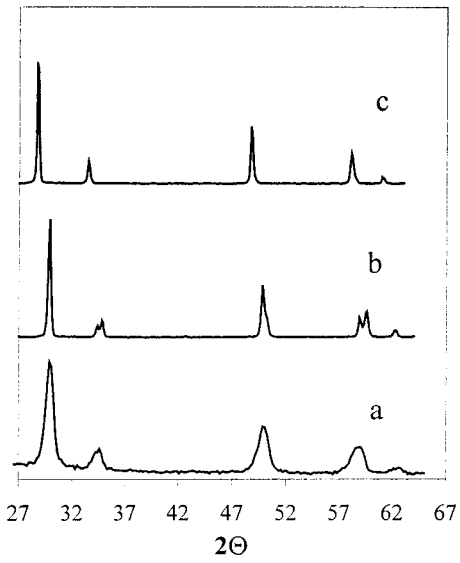

Figure 1. XRD patterns of (a) $Y_{0.05}Ce_{0.1}Zr_{0.85}O_2$ calcined at 823 K, (b) $Y_{0.05}Ce_{0.1}Zr_{0.85}O_2$ calcined at 1743 K, and (c) $Y_{0.1}Ce_{0.1}Zr_{0.8}O_2$ samples calcined at 1743 K.

phase in $Y_{0.05}Ce_{0.1}Zr_{0.85}O_2$ with the cubic phase whereas the $Y_{0.1}Ce_{0.1}Zr_{0.8}O_2$ solid corresponds only to the cubic phase.[16]

1.2. TPR. TPR profiles of $Y_{0.05}Ce_{0.1}Zr_{0.85}O_2$ and $Y_{0.1}Ce_{0.1}Zr_{0.8}O_2$ samples are illustrated in Figure 2A and Table 1. The curves obtained consist of two poorly resolved peaks whose position and area reflect the OSC of samples. The low-temperature (LT $\approx$ 680 °C) peak was attributed to the reduction of the surface Ce^{4+} ions and the high-temperature (HT) peak was associated with the reduction of CeO_2 in the bulk.[3,6,14] These results indicate that the $Y_{0.1}Ce_{0.1}Zr_{0.8}O_2$ solid is more reducible (858 K) than the $Y_{0.05}Ce_{0.1}Zr_{0.85}O_2$ one (881 K). In addition, compared to a $Ce_{0.2}Zr_{0.8}O_2$ solid, the reduction of solids doped with yttrium was performed at less than 174 and 197 K, respectively, than that obtained for the solid without yttrium (1032 K). Therefore, the introduction of the yttrium additive essentially improved the redox properties change of the CeO_2-ZrO_2 system and confirmed our supposition concerning the enhanced oxygen mobility by reduction treatment in the $Y_{0.05}Ce_{0.1}Zr_{0.85}O_2$ and $Y_{0.1}Ce_{0.1}Zr_{0.8}O_2$ solids.

The analysis of the shape of overlapped peaks by means of approximation by Gauss functions with the subsequent integration has allowed sharing of the peaks and estimating of the contribution of each one (Figure 2B). So it was found that the $Y_{0.1}Ce_{0.1}Zr_{0.8}O_2$ sample is characterized by a greater OSC. It follows from a comparison of the HT-peak areas for two supports expressed in the amount of hydrogen necessary for reduction of 1 g of the solid solution (Table 1).

Thus, the increased mobility of lattice oxygen by reduction treatment and its quantity is observed for the $Y_{0.1}Ce_{0.1}Zr_{0.8}O_2$ sample crystallizing in the cubic modification as compared to the $Y_{0.05}Ce_{0.1}Zr_{0.85}O_2$ sample whose structure represents a mixture of the tetragonal and cubic phases. It is good confirmation that the high defective cubic structure of the $Y_2O_3-CeO_2-ZrO_2$ solid solutions favors high OSC.

(16) Lin, J.-D.; Duh, J.-G. *J. Am. Ceram. Soc.* **1998**, *81*, 853.

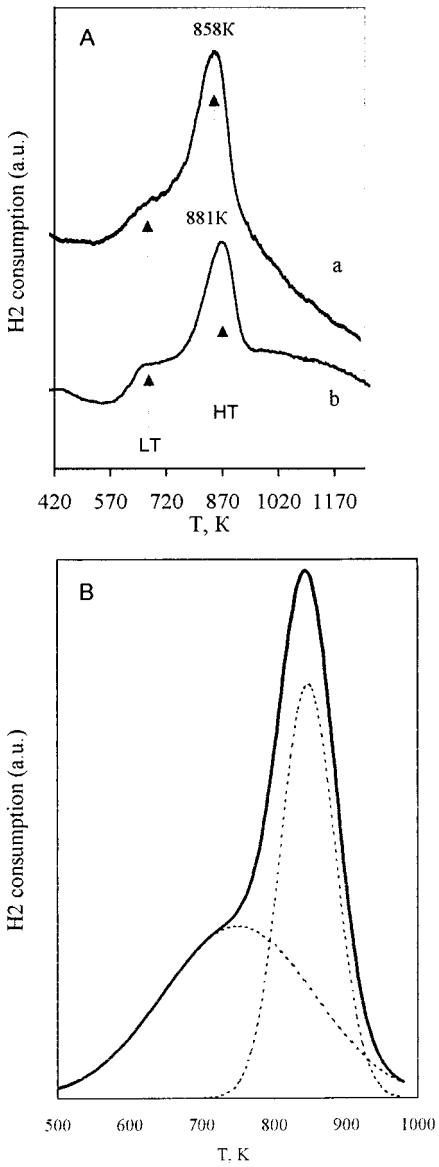

Figure 2. (A) TPR profiles of (a) $Y_{0.05}Ce_{0.1}Zr_{0.85}O_2$ and (b) $Y_{0.1}Ce_{0.1}Zr_{0.8}O_2$ samples; (B) calculated TPR peak areas after the correction of the baseline.

Table 1. Specific Area (S_{sp}), TPR Data, and H_2 Consumption

sample	S_{sp}, $m^2\,g^{-1}$	TPR peaks, K	H_2 uptake, mmol g^{-1}
$Y_{0.05}Ce_{0.1}Zr_{0.85}$	60	~668; 881	0.120
$Y_{0.1}Ce_{0.1}Zr_{0.8}$	65	~668; 858	0.208
0.5%Cu/$Y_{0.1}Ce_{0.1}Zr_{0.8}$	55	435; 835	0.271
1%Cu/$Y_{0.1}Ce_{0.1}Zr_{0.8}$	43	430; 440; 832	0.337
3%Cu/$Y_{0.1}Ce_{0.1}Zr_{0.8}$	38	412; 429; 482; 821	0.636

2. y%$CuY_xCe_{0.1}Zr_{0.9-x}O_2$. 2.1. DRES. Figure 3 shows the UV−vis spectra of y%$CuY_xCe_{0.1}Zr_{0.9-x}O_2$ samples previously calcined at 623 K. The increasing concentration of entered copper was not accompanied by a proportional (1:2:6) increase of intensity of the absorption band attributed to the d−d transitions at the Cu^{2+} ions, confirming the decreasing Cu_{isol}/Cu_{total} value. Three absorption bands were observed in the spectra: the first one situated at 12 000−14 000 cm^{-1} can be attributed to d−d transition in Cu^{2+} ions located in sites with octahedral symmetry;[17,18] the second one, characterized by a weak absorption band and centered at 20 000 cm^{-1},

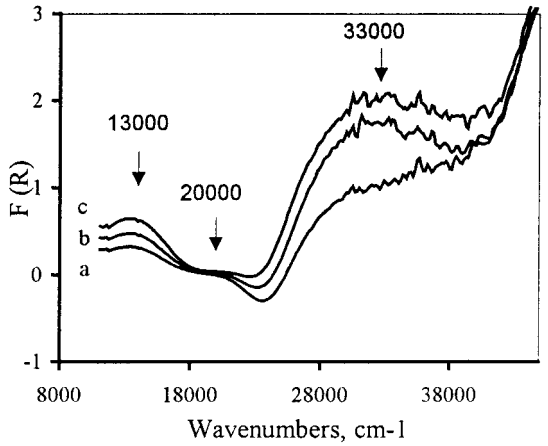

Figure 3. UV−visible spectra of (a) 0.5%$CuY_{0.1}Ce_{0.1}Zr_{0.8}O_2$, (b) 1%$CuY_{0.1}Ce_{0.1}Zr_{0.8}O_2$, and (c) 3%$CuY_{0.1}Ce_{0.1}Zr_{0.8}O_2$.

can be related to the appearance of large X-ray amorphous CuO aggregates (were not detected by the XRD) poorly interacting or not interacting with the support.[19] The third one observed at 32 000−35 000 cm^{-1} can be due to electron transfer from the orbital of the O^{2-} ligand to the vacant d-orbital of Cu^{2+} ions in small clusters.[20] As a rule, such transitions are displayed in a range from 26 000 cm^{-1} up to 30 000 cm^{-1}. The high-frequency shift of this band in our case can be caused by the occurrence of strong metal−support interaction, which as is known,[21−22] takes place in similar systems. Such interactions result in the increasing of splitting between appropriate electron levels and, as a consequence, in increasing energy (frequency) of transition.

2.2. EPR. Figure 4a shows the EPR spectrum of the 0.5%$CuY_xCe_{0.1}Zr_{0.9-x}O_2$ sample previously calcined at 723 K and subsequently outgassed at the same temperature. The spectrum represents an axial anisotropy of the **g** tensor and not well-resolved hyperfine structure (HFS). The spectrum is unambiguously due to the interaction of free electrons of Cu^{2+} ($3d^9$) with the magnetic nuclear moment of copper ($I = 3/2$) that gives rise to a 4-fold hyperfine splitting of all the anisotropic components. The values of integrated intensity of signals testified to the observation of practically all entered copper. It also followed from equality of intensities of signals for vacuum-treated and oxidized samples. The not well-resolved hyperfine structure is due to the strong dipolar interaction between the Cu^{2+} ions.

The signal with the EPR parameters values $g_{\|} = 2.24$, $A_{\|} = 153$ G, $g_{\perp} = 2.05$, $A_{\perp} = 15$ G, and $g_{iso} = 2.112$ is characteristic of Cu^{2+} ions located in octahedral symmetry sites tetragonally distorted and surrounded by more than six ligands.[18,23] These results are in agreement with data of the DRES method. In fact, the

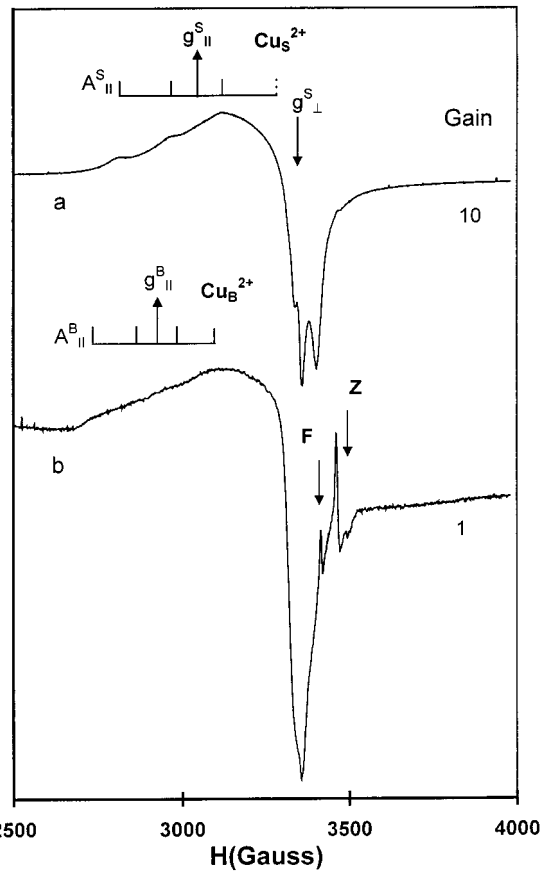

Figure 4. EPR spectra of 0.5%$CuY_{0.1}Ce_{0.1}Zr_{0.8}O_2$ sample (a) previously calcined at 723 K and subsequently outgassed at the same temperature and (b) after the soft CO reduction.

absorption band observed at 12 000−14 000 cm^{-1} for y%$CuY_xCe_{0.1}Zr_{0.9-x}O_2$ is characteristic of Cu^{2+} ions in octahedral symmetries (Figure 3).

For low copper contents (<3%), the enhancement of the deposited metal content was accompanied by increasing of the copper(II) signal and broadening of the components of the hyperfine structure due to a dipole−dipole interaction and then the formation of clusters or/and small particles of CuO. For high copper contents (3%), the decrease of the signal intensity can be explained by the formation of CuO aggregates on the solid surface. These latter species are undetectable in the EPR technique; this is due either to the strong dipolar interaction between the Cu^{2+} ions or to the antiferromagnetic character of the solid.

In conclusion, the EPR technique evidenced two types of Cu^{2+} species in y%$CuY_xCe_{0.1}Zr_{0.9-x}O_2$ solids: isolated Cu^{2+} ions and cluster of copper(II) or/and small particles of CuO. All these species are rather located on the solid surface.

2.3. TPR. The addition of copper to the $Y_xCe_{0.1}Zr_{0.9-x}O_2$ solids, resulted in the appearance of new peaks in the range of 400−500 K after the TPR treatment (Figure 5 and Table 1), whereas the TPR peaks already obtained for $Y_{0.05}Ce_{0.1}Zr_{0.85}O_2$ (881 K) and $Y_{0.1}Ce_{0.1}Zr_{0.8}O_2$ (858 K) solids were shifted to low temperatures in the presence of copper. The shift was more and more

(17) Choisnet, J.; Cornet, D.; Hemidy, J. F.; Nguyen, N.; Dat, Y. *J. Solid State Chem.* **1981**, 40.
(18) Dergaleva, G. A.; Pahomov, N. A.; Bendyurin, V. N.; Anufrienko, V. F. *Kinet. Katal.* **1991**, *32*, 490.
(19) Sengupta, G.; Chakraborty, A.; Banerjee, S.; Das, D. P.; Choudhury, R. P.; Banerjee, R. K.; Sanyal, R. M. *Appl. Catal.* **1991**, *68*, 1.
(20) Aboukaïs, A.; Bechara, R.; Aïssi, C. F.; Bonnelle, J. P.; Ouqour, A.; Loukah, M.; Coudurier, G.; Vedrine, J. C. *J. Chem. Soc., Faraday Trans.* **1993**, *89*, 2545.
(21) Zhou, R. X.; Jiang, X. Y.; Mao, J. X.; Zheng, X. M. *Appl. Catal.* **1997**, *162*, 213.
(22) Kundakovic, Lj.; Flytzani-Stepanopoulos, M. *Appl. Catal.* **1998**, *171*, 13.
(23) Crusson-Blouet, E.; Aboukaïs, A.; Aïssi, C. F.; Guelton, M. *Chem. Mater.* **1992**, *4*, 1129.

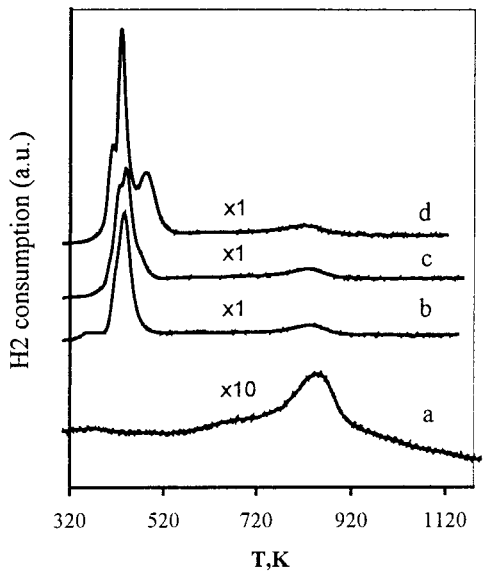

Figure 5. TPR profiles of (a) $Y_{0.1}Ce_{0.1}Zr_{0.8}O_2$, (b) $0.5\%CuY_{0.1}Ce_{0.1}Zr_{0.8}O_2$, (c) $1\%CuY_{0.1}Ce_{0.1}Zr_{0.8}O_2$, and (d) $3\%CuY_{0.1}Ce_{0.1}Zr_{0.8}O_2$.

significant while the copper concentration increased. This means that the reduction of Ce^{4+} in the solid bulk is easier in the presence of copper and leads to the increase of oxygen mobility of the solids.

In the range of 400−500 K, a single peak was observed at 435 K for the $0.5\%CuY_{0.1}Ce_{0.1}Zr_{0.8}O_2$ solid and two peaks (430 and 440 K) for $1\%CuY_{0.1}Ce_{0.1}Zr_{0.8}O_2$ and three (412, 429, and 482 K) for $3\%CuY_{0.1}Ce_{0.1}Zr_{0.8}O_2$. The integration of corresponding peaks has shown that the H_2 consumption increased with copper concentration (Table 1). This phenomenon can confirm that the peaks observed are due to the presence of copper(II) species in the solids. On the basis of the literature data,[24−28] these TPR peaks can be associated with the reduction of support and Cu^{2+} species. The peak obtained at 435 K for the $0.5\%CuY_{0.1}Ce_{0.1}Zr_{0.8}O_2$ was attributed to the reduction of Ce^{4+} ions present on the $Y_{0.1}Ce_{0.1}Zr_{0.8}O_2$ surface. When the concentration of copper increases in the solid, the peak shifted to 430 and 412 K for $1\%CuY_{0.1}Ce_{0.1}Zr_{0.8}O_2$ and $3\%CuY_{0.1}Ce_{0.1}Zr_{0.8}O_2$, respectively, indicating then that the reduction of the Ce^{4+}/surface became easier. Indeed, it has been demonstrated[28] that the presence of copper in cerium zirconium oxides increases the reducibility of the solid surface particularly when these species are present in the solid in the form of isolated and clusters/small particles and not in the form of aggregates. This hypothesis can explain why the peak obtained at 435 K shifts to low reduction temperature when the copper concentration increased. To notice that the shift at low temperature reduction is not directly proportional to the copper content (Table 1), this can be due to the simultaneous formation of CuO aggregates with the isolated and clusters/small particles of Cu^{2+} species. The formation of such aggregates can be confirmed by the diminution of the specific area of solids (Table 1). The peaks obtained at 440 and 429 K for $1\%CuY_{0.1}Ce_{0.1}Zr_{0.8}O_2$ and $3\%CuY_{0.1}Ce_{0.1}Zr_{0.8}O_2$, respectively, can be attributed to the reduction of Cu^{2+} ions in the form of isolated and clusters/small particles, whereas the peak obtained at 482 K for $3\%CuY_{0.1}Ce_{0.1}Zr_{0.8}O_2$ is attributed to the reduction of CuO in the form of aggregates. These results are closely related to those obtained by EPR. To confirm the copper sites location in the solid, a soft reduction of $y\%CuY_{0.1}Ce_{0.1}Zr_{0.8}O_2$ was performed under a CO gas flow.

The treatment of samples by hydrogen resulted in the total disappearance of the Cu^{2+} ions EPR signals, testifying to a complete reduction of copper(II) species into Cu^+ or/and Cu°. On the contrary, the soft reduction treatment by CO at room temperature resulted in a disappearance of the EPR signal already attributed to Cu^{2+} ions located on the solid surface, whereas three new signals assigned by B, Z, and F appeared (Figure 4b).

The signal, assigned by B and characterized by the following EPR parameters, $g_{\|} = 2.3$, $A_{\|} = 115$ G, $g_{\perp} = 2.05$, $A_{\perp} = 12$ G, and $g_{iso} = 2.112$, was attributed to Cu^{2+} ions remaining in the solid after that soft CO reduction. These species ought be located in the solid bulk to be protected from that reduction. From the EPR parameters values, these Cu^{2+} ions are situated in octahedral symmetry sites with strong distortions; indeed, Ermakovich[29] has found similar EPR parameter values for Cu^{2+} ions doped in the $(HfO_2)_{0.9}(Y_2O_3)_{0.1}$ cubic phase. The intensity of the B signal increased with the Cu^{2+} ions concentration (Figure 5b). Since a soft reduction cannot reduce or totally reduce the Cu^{2+} ions located in the solid bulk, this can explain the increase of such species with the copper concentration in the solid.

The Z signal represents an axial symmetry ($g_{\perp} = 1.975$; $g_{\|} = 1.956$) as it was already described by different authors and assigned to Zr^{3+} ions.[30,31] The **g** values are in agreement with the expected ones for a d^1 ion in an octahedral environment with strong tetragonal distortion. The formation of Zr^{3+} species is due to the reduction by CO of the Zr^{4+} into Zr^{3+} species. Indeed, Chen et al.[31] have suggested that the formation of Zr^{3+} ions in the sulfated zirconia are due to the reduction by SO_4^{2-} of the Zr^{4+} into Zr^{3+} species.

The F signal, centered at $\mathbf{g} = 2.001$, with a peak-to-peak width equal to 7 G, was attributed to trapped electrons in the $y\%CuY_{0.1}Ce_{0.1}Zr_{0.8}O_2$ matrix. Similar signals,, have been obtained by numerous authors[32] and have been attributed to F centers, that is, electrons stabilized in oxygen vacancies.

The analysis of the IR spectrum of CO adsorbed on samples with 0.5 and 1% Cu content at 323 K (Figure 6) has shown that copper was found mainly in the reduced state. This is proved with the high intensity of

(24) Terribile, D.; Trovarelli, A.; De Leitenburg, C.; Primavera, A.; Dolcetti, G. *Catal. Today* **1999**, *47*, 133.
(25) Fornasiero, P.; Kašpar, J.; Sergo, V.; Graziani, M. *J. Catal.* **1999**, *182*, 56.
(26) Fornasiero, P.; Kašpar, J.; Graziani, M. *J. Catal.* **1997**, *167*, 576.
(27) Hickey, N.; Fornasio, P.; Kašpar, J.; Graziani, M.; Blanco, G.; Bernal, S. *Chem. Commun.* **2000**, 357.
(28) Courtois, X. Thesis, University of Claude Bernard, Lyon 1, France, **2000**.
(29) Ermakovich, K. K. *Russ. J. Phys. Solid State* **1976**, *18*, 1450.
(30) Morterra, C.; Giamello, E.; Orio, E.; Volante, M. *J. Phys. Chem.* **1990**, *94*, 3111.
(31) Chen, F. R.; Coudurier, G.; Joly, J. F.; Vedrine, J. C. *J. Catal.* **1993**, *143*, 616.
(32) Lopez, T.; Tzompantzi, F.; Navarrete, J.; Gomez, R.; Boldu, J. L.; Munoz, E.; Novaro, O. *J. Catal.* **1999**, *181*, 285.

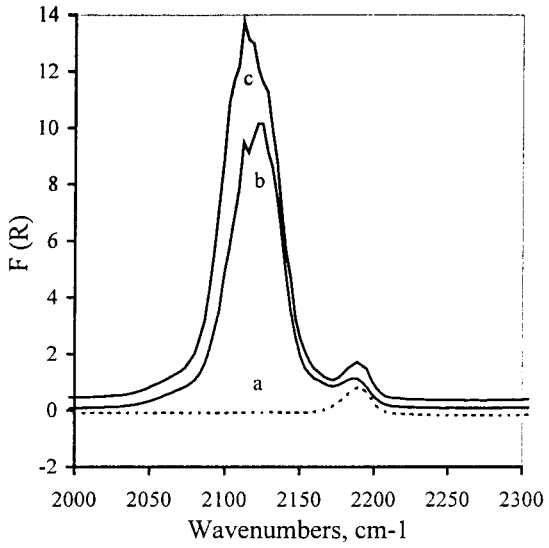

Figure 6. IR spectra of CO adsorbed on (a) $Y_{0.1}Ce_{0.1}Zr_{0.8}O_2$, (b) 0.5%$CuY_{0.1}Ce_{0.1}Zr_{0.8}O_2$, and (c) 1%$CuY_{0.1}Ce_{0.1}Zr_{0.8}O_2$.

the absorption bands attributed to Cu^+ ions ($\nu \approx 2130$ cm^{-1}) and clusters of Cu^0 with electronic density partially shifted to the support, Cu_n^+ ($\nu \approx 2110$ cm^{-1}).[33,34]

Thus, in the thermally treated and oxidized samples the copper is present in three forms: as the isolated ions Cu^{2+}, the small copper clusters, and the larger X-ray amorphous CuO particles. The isolated Cu^{2+} ions and the small clusters showed higher reduction ability (both concerning hydrogen and CO) in comparison with bulk-like CuO particles.

Conclusion

In this work, it has been demonstrated that the reducibility properties of the $Y_xCe_{0.1}Zr_{0.9-x}O_2$ solids ($x = 0.5$ and 0.1) depend on the yttrium contents. The addition of copper(II) on these solids enhanced more the reduction of Ce^{4+} ions present on the surface and in the bulk of the solid. The copper species are located in the solids in the form of isolated Cu^{2+} ions and small particles of CuO.

Taking into account high oxygen mobility by reduction treatment of supports and the occurrence of low-temperature oxygen-free oxidation of CO (EPR, IRS), providing participation in the process not only easily reducible copper species but also oxygen of support (TPR), it is possible to expect that the y%$CuY_{0.1}Ce_{0.1}Zr_{0.8}O_2$ samples, investigated by us, will appear to be active TWCs, especially under cold-start conditions, that is, under conditions of high CO concentration, absence of O_2, and low temperatures.

Acknowledgment. The authors would like to thank the "Conseil Général du Nord", the "Région Nord-Pas de Calais", and the European Community (European Regional Development Fund) for financial support in the EPR apparatus purchase. The authors also thank INTAS for grants under which this work was carried out.

CM000636P

(33) Davydov, A. A.; Budneva, A. A.; Sokolovskii, V. D. *Kinet. Katal.* **1989**, *30*, 1407.
(34) Hadjiivanov, K. I.; Kantcheva, M. M.; Klissurski, D. G. *J. Chem. Soc., Faraday Trans.* **1996**, *92*, 4595.